euspen's 23rd International Conference & Exhibition, Copenhagen, DK, June 2023
www.euspen.eu

Accounting for elastic recovery during micro-scratching of a brittle material in the ductile regime

Yan Jin Lee and Hao Wang*

Department of Mechanical Engineering, College of Engineering and Design, National University of Singapore

**mpewhao@nus.edu.sg*

Abstract
Elastic recovery is prevalent in metal cutting with a well-known association to hinder the geometrical accuracy of the machined feature. Yet, consideration for such a downside is rarely considered in the micro-cutting of brittle materials, which should manifest strongly during cutting in the ductile regime. This paper performed plunge and orthogonal micro-scratching on a brittle material (calcium fluoride) where the penetration and residual depth information were collected to reveal the magnitude of elastic recovery. The degree of recovery was found to be depth-dependent with an association to size effects. Additionally, plunge scratching produced results that differed from orthogonal scratching in terms of penetration and residual depths alongside different trends relative to scratching speed. The findings identify critical areas for further investigation in determining the relationship between size effects and elastic recovery, and the potential need to revisit experimental methodologies employed for studing the micro-cutting of brittle materials.

Precision manufacturing, ductile–brittle transition, calcium fluoride, anisotropy, elastic recovery

1. Introduction

Advances in precision manufacturing have enabled micro-cutting of optical-grade surfaces on brittle ceramics [1]. This is only achievable with ductile-mode cutting that is the cutting conditions capable of producing defect free surfaces (typically depicted as crack-free). Within the ductile regime, elastic strain energy is converted into plastic energy through plastic deformation (observed through cutting chips when machining ductile materials) [2]. Upon release of the tool-workpiece contact at the cutting zone, the remaining stored elastic energy is dissipated through elastic recovery by means of a reversion of the machined surface to its original level. As most of the cutting energy had already been converted to plastic energy, dissipation of remnant stored elastic energy results in only partial recovery of the machined surface.

This recovery can hinder machining accuracies when the designed surface (e.g., a groove) elastically recovers [3]. The problem is well-known to occur in metal cutting due to the observable magnitudes of recovery. However, such occurrences are rarely reported for brittle materials due to the postulated dissipation of elastic energy into surface generation in the form of micro-cracks [4]. As this work limits the discussion to brittle materials within the ductile regime, the magnitude of elastic recovery cannot be ignored.

The ductile regime of brittle materials in terms of the critical uncut chip thickness is typically < 1 µm. At this length scale, various size effects have been identified such as the grain size effect (for polycrystals) and the indentation size effect [5], where large differences in material properties manifested. Thus, a constant elastic spring-back value cannot be expected during cutting of brittle materials at this length scale, and it is important to reveal relationships between cutting depths and the magnitude of elastic recovery.

Plunge-cutting is a common technique to determine the critical uncut chip thickness of a material that defines the ductile and brittle regimes [6]. Thus, this paper investigates the use of this technique to provide additional information in determining potential depth-dependent elastic recovery of the deformed surface.

The material in-focus in this work is single-crystal calcium fluoride (CaF_2), which is an optical material germane for a long list of applications due to its wide optical transmissivity, low birefringence, and low refractive index. These properties make it meaningful to study the machinability of this material [7]. While it is inherently brittle with a low fracture toughness, ductile-mode cutting has been successfully achieved in multiple works [8,9]. Yet, little has been reported about the elastic recovery occurring on its machined surfaces, which will be uncovered in this paper. For this work, a micro-scratching setup will be employed to investigate the elastic recovery with specially designed capabilities integrated within the system to gain better understanding of the material properties during deformation in the micro-scale.

2. Experiments

Micro-scratching tests were performed on a MCT^3 instrumented micro-scratch machine from Anton Paar (Figure 1). The scratch setup included a 100 µm radii conical indenter tip attached to in-built force and acoustic emission (AE) sensors. A CaF_2 sample with the (111) top plane was mounted on a sample holder fixed to the motorized stage of the MCT^3, which controlled the scratch position and performed the scratch along the $[\bar{2}11]$ direction by pushing the sample into the indenter and providing the linear scratch motion. Two types of scratch tests were performed for this study: (i) plunge scratching and (ii) orthogonal scratching.

The ductile–brittle transition (DBT) in micro-scratching was first characterized by plunge scratching to determine the

conditions to achieve ductile-mode scratching. Here, the indenter scratched the sample by linearly increasing the applied load from 0–1 N as the indenter traversed across the scratch length of 1 mm.

Orthogonal scratching was subsequently performed by applying constant loads in the ductile regime where the loads were selected to be -10% and -20% of the determined DBT. Four different scratch speeds were employed (50, 100, 150, 200 mm/min) and three scratches were performed for each type of test to ensure repeatability of the results and to obtain averaged values.

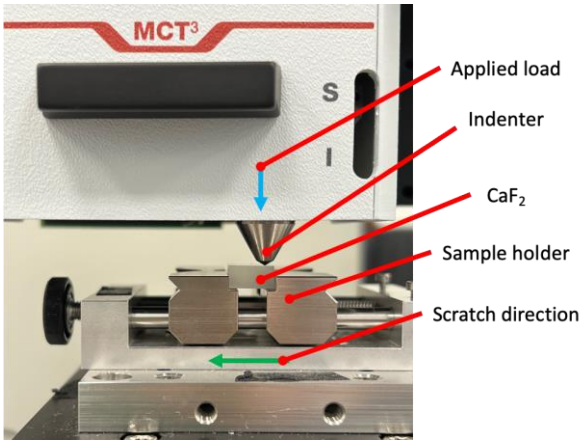

Figure 1. Micro-scratching setup

In both types of scratches, a pre- and post-scan of the intended scratch location were performed to correspondingly determine the initial sample surface position and the residual depth of the scratch after elastic recovery. A low load of 0.03 N was applied to the indenter as it performed the scans inducing minimal damage to the sample. The penetration depth of the indenter was also concurrently measured during the actual scratch, which provided the necessary information for observation of elastic recovery. AE signals were also captured during the scratches picking up intensities resonating at a frequency of 150 kHz (a typical value to pick up the formation of micro-cracking). Optical images and measurement of the groove profiles were performed using a laser confocal microscope (Olympus LEXT OLS-5000).

3. Results and discussion

3.1. Elastic recovery in the ductile regime

The transition between ductile- and brittle-mode scratching was determined by optical observation of the onset of cracking along the scratched surface as the scratch load progressively increased. Figure 2(a) presents the top-view optical images of the grooves and the location of the DBTs that correspond to an approximate critical load of 0.5 N across the different scratch speeds. Figure 2(b) also presents the acoustic emission (AE) measurements during the scratches, which indicate crack formations with the rise in acoustic detection at applied loads above 0.5 N. As the scratches continue to plunge deeper into the sample, the quantity and size of cracks increase and emit more sound waves from the generation of new surfaces. Therefore, the subsequent constant load scratching tests were set at 0.45 and 0.4 N corresponding to -10% and -20% lower loads that ensure grooves produced under ductile-mode scratching.

Figure 3 plots the averaged penetration depths (Pd) and residual depths (Rd) for the different scratch speeds, which are used to determine the elastic recovery of the surface (Equation 1). In the early stages of the scratch, the scratched surface exhibited a near-full recovery (80-90%) but the degree of elastic recovery dropped and stabilized at approximately 65% as the penetration depth increased further as shown in Figure 3. The erratic fluctuations in the early stages of the scratch can be associated with pop-in effects at that deformation length scale where sudden bursts of strain may occur due to the nucleation of dislocations [10]. While this happens, applied forces are also released, which therefore gives irregular measurements at the initial stages of the scratch.

The elastic recovery showed a non-linear decline in the ductile regime and coincidentally stabilized after reaching the DBT at 0.5 N. While it may appear convenient to suggest that the elastic recovery changes with different scratch depths in the ductile regime, the indentation size effect [5] is also known to affect the mechanical properties of the material at this length scale. This refers to the size-dependent hardness or strength of the material where observations of increased strength were reported at smaller deformation scales on CaF_2 [10].

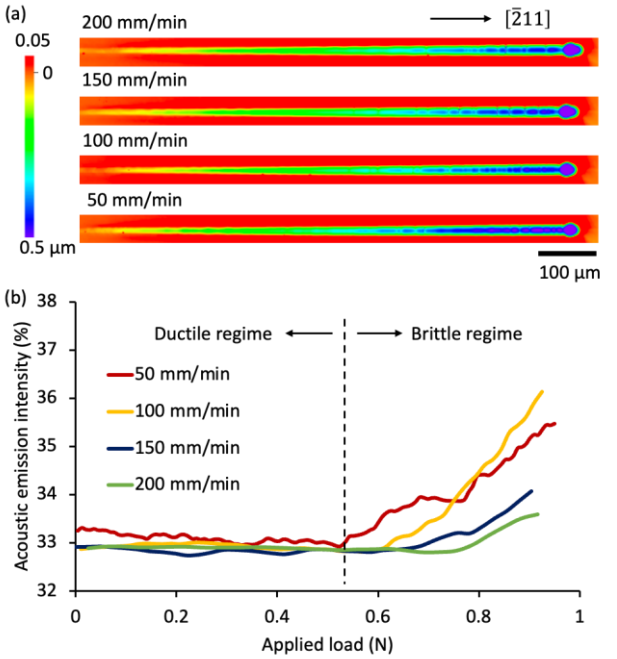

Figure 2. Determining the ductile–brittle transitions (DBTs): (a) Top-view optical images of the scratched grooves; (b) acoustic emission (AE) signal intensity measurements

$$E_r = \frac{P_d - R_d}{P_d} \quad (1)$$

To understand the influence of the size effect, the effective stress required to cause yielding of the material must be determined. The cross-section of the groove is drawn in Figure 4(a), which assumes that elastic recovery occurs unidirectionally upwards such that the surface within the groove of the residual depth represents the plastic zone and the surfaces on the outer rim of the groove represents the recoverable elastic zone. In other words, the applied stresses located at the edges of the residual depth groove are assumed to represent the representative strength of the material for that deformation length scale (Figure 5). The material may recover along directions perpendicular to the arc of the grooves, but the model presented in this paper assumes a more simplified representation for a qualitative understanding of the recovery. Further development in the analytical model would be necessary to precisely determine the stress distribution along the cross-sectional area of the groove.

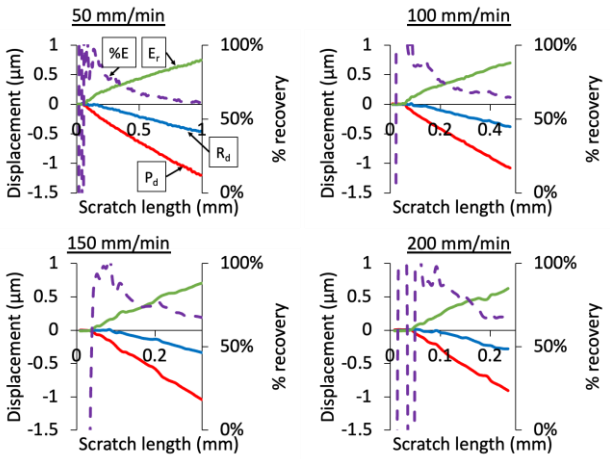

Figure 3. Penetration (P_d) depth, residual (R_d) depth, elastic recovery (E_r), and magnitude of recovery (%E) during progressive loading scratching

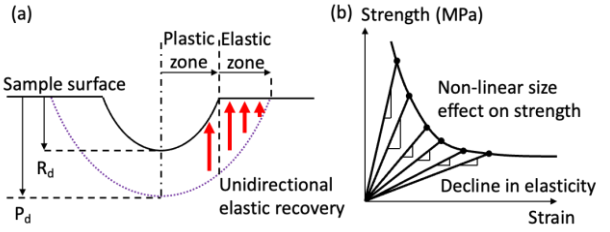

Figure 4. (a) Cross-section of a groove and the corresponding elastic and plastic regions; (b) representation of elasticity while considering size effects

Having clarified the assumptions to simplify the problem, the applied stress across the arc length of the groove can be calculated in Equation 2. It is important to further note that this calculation does not represent the actual applied stress as it only accounts for the two-dimensional arc length and gives a representative stress value, which is sufficient for the discussion of this paper. The defining stress at the position of the groove that separates the elastic and plastic regions can be calculated in Equation 3 and is plotted in Figure 5. It is expected that the representative strength of the material progressively declines with increasing scratching depth alike the indentation size effect on hardness [11]. It is also interesting to note that the representative strength levels out to a constant value at applied loads between 0.5–0.6 N, which coincides with the region where the elastic recovery became a constant. From this, it is suggestive that the observed change in elastic recovery is not due to depth-dependency but rather the size effect on material strength. The high strength at low scratch depths would suggest that the elasticity would also be high for the correspondingly low strain (Figure 4(b)).

$$\sigma = \frac{F_n}{2r_n \operatorname{acos}\left(\frac{r_n - P_d}{r_n}\right)} \tag{2}$$

$$\sigma_p = \frac{\sigma(P_d - R_d)}{\frac{\pi}{2} P_d \sqrt{P_d(2r_n - P_d)}} \tag{3}$$

where F_n is the applied force and r_n is the indenter radius.

3.2. Correlation with constant depth scratching

With the known DBT, orthogonal scratching at -10% and -20% loads produced crack-free grooves in the ductile regime (Figure 6). The corresponding average penetration and residual depths are shown in Figure 7(a). The depths measured in orthogonal scratching are larger than that recorded in plunge scratching. Additionally, the depths decrease with increasing scratch speed during plunge scratching. These observations are potentially due to the different orientation of material deformation, particularly with respect to the anisotropic properties of a single crystal where different orientations of applied loads (Figure 7(b)) will result in different degrees of deformation according to the activation of the $\{001\} < 1\bar{1}0 >$ primary slip system. The increase in scratch speed is related to the increase in strain rate, which again is correlated with the crystallographic-dependent dislocation activity. In this case, dislocation motion may be hindered and discourage plasticity during plunge scratching, and dislocations were unable to keep up with the strain rate, thus resulting in lower degrees of deformation.

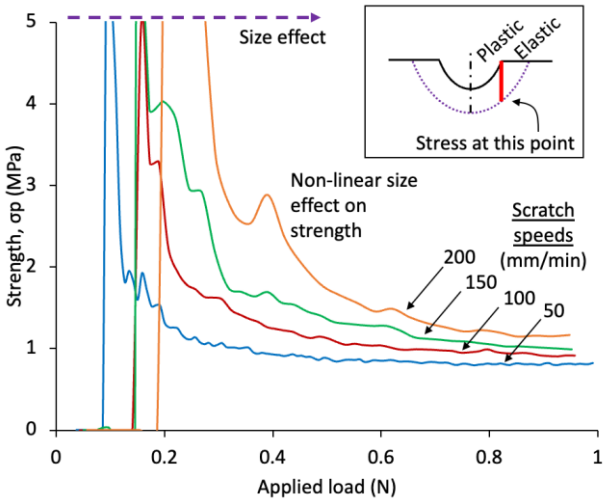

Figure 5. Representation of the material strength at the intersection between the elastic and plastic regions

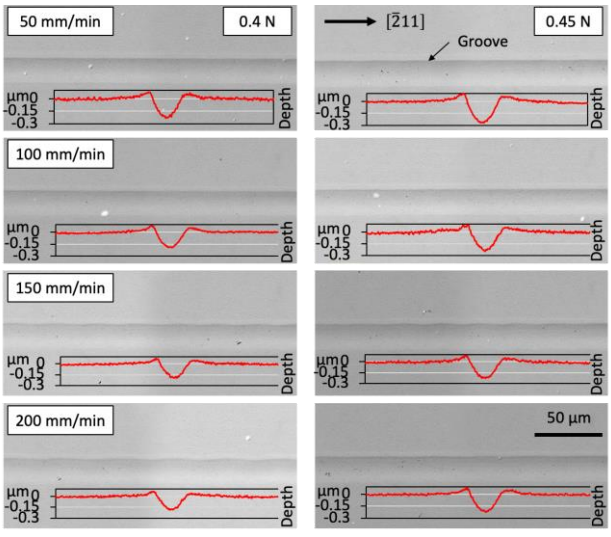

Figure 6. Top view of crack-free orthogonal grooves produced along the [$\bar{2}$11] orientation in the ductile regime and the corresponding cross-sectional profile

Figure 8 plots the elastic recovery comparison between plunge and orthogonal scratching. The -10% and -20% bars correspondingly show higher elasticity as attributed to the size effect in Figure 3. While the depth profiles of the orthogonal scratches (Figure 7) are higher than the plunge scratches, the elastic recovery consistently shows the contrary (Figure 8). Again, this is reasoned with the differences in loading

orientations where anisotropic properties of the single crystal account for the differences in elastic recovery. As the material deforms differently during scratching, different degrees of recovery can also be expected. Elastic recovery is also observed to increase with scratching speed and can be reasoned with the rate of loading and unloading. At higher scratch speeds, the work material has lesser contact time and lower restrictions to recover and therefore gives higher degrees of elastic recovery across the different types of scratches.

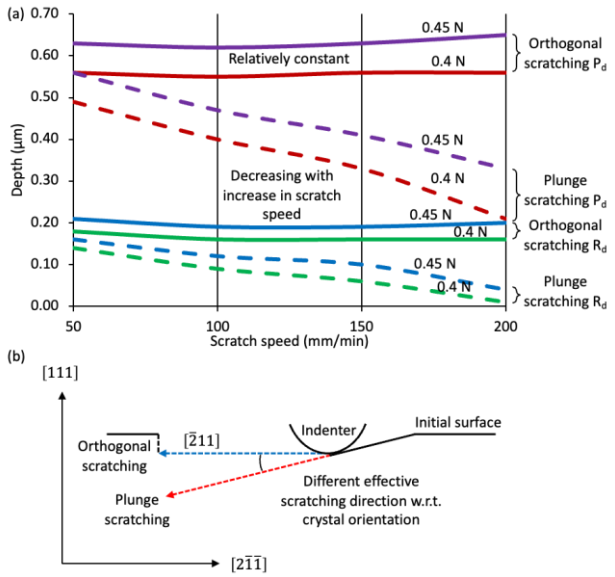

Figure 7. Comparison of penetration and residual depths between orthogonal and plunge scratching: (a) line plot of the average depths; (b) schematic for the orientation-dependent loading/scratching conditions

The line plots in Figure 8 depict the relationship between the elastic recovery at -20% (0.4 N) and -10% (0.45 N) loads for both orthogonal and plunge scratching by determining the ratio of the plunge/orthogonal elastic recovery. The plots show that the elastic recovery for 0.4 N during plunge scratching increases with scratching speed at a much higher rate than that in orthogonal cutting. This phenomenon is however not observed for the higher 0.45 N load that shows more linearity. It indicates that the combination of lower loads under the size effect and higher scratch speeds should result in higher degrees of elastic recovery.

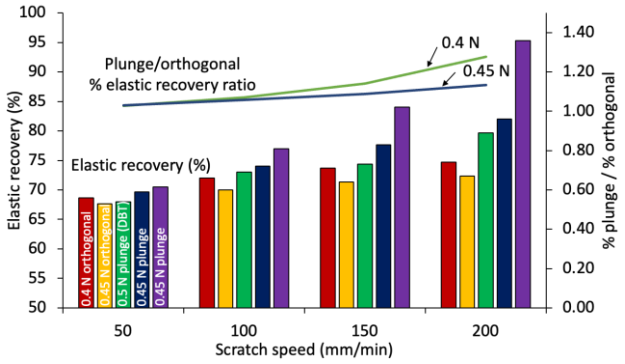

Figure 8. Comparison in elastic recovery between orthogonal and plunge scratching

4. Conclusions

This investigation acknowledges the importance of considering the elastic recovery of a machined surface in precision manufacturing and employed plunge scratching on calcium fluoride single crystal as a method to understand the phenomenon in the ductile regime. Two key observations were made in this work:

1. Elastic recovery in the ductile regime is depth-dependent but is attributed to the size effect on the material strength.
2. The anisotropy of the single crystal gives inaccurate representations of the scratching results (i.e., penetration depth, residual depth, and elastic recovery) when using plunge scratching to associate with orthogonal scratching.

Therefore, further studies are necessary to investigate the correlation between the size effect and the elastic recovery to provide more predictable estimations of its magnitude, which will be useful for tool path planning during micro-cutting. Additionally, the differences in results between plunge and orthogonal scratching opens the question on the accuracy of plunge cutting as a method to determine critical cutting parameters (e.g., cutting speed, critical uncut chip thickness, etc.). Such a question should be revisited to have a more accurate understanding on the material-dependent characteristics for efficient precision manufacturing.

Acknowledgements

This work is proudly supported by Singapore Ministry of Education AcRF (Grant nos.: MOE-T2EP50220-0010 and MOE-T2EP50120-0010) and Agency for Science, Technology and Research, Singapore (Grant no.: A19E1a0097).

References

[1] Tan N Y J, Zhang X, Neo D W K, Huang R, Liu K, Kumar A S 2021 *J. Manuf. Process.* **71** 113-133
[2] Wang H, To S, Chan C Y, Cheung C F, Lee W B 2010 *Int. J. Mach. Tools Manuf.* **50** 9-18
[3] Huang X, Wan Z, Luo Y, Qing J, Yang S 2023 *Wear* **516-517** 204622
[4] Huang N, Yan Y, Zhou P, Kang R, Guo D, Goel S 2020 *Precis. Eng.* **65** 64-71
[5] Nix W D and Gao H J 1998 *J. Mech. Phys. Solids.* **46** 411-25
[6] Lee Y J and Wang H 2021 *Ceram. Int.* **47** 28543-28556
[7] Lee Y J, Kumar A S, Wang H 2021 *Int. J. Mach. Tools Manuf.* **168** 103787
[8] Mizumoto Y and Kakinuma Y 2018 *Precis. Eng.* **53** 9-16
[9] Wang H, Riemer O, Rickens K and Brinksmeier E 2016 *Scr. Mater.* **115** 21-6
[10] Lodes M A, Hartmaier A, Göken M and Durst K 2011 *Acta Mater.* **59** 4264-73
[11] Chua J, Zhang R, Chaudhari A, Vachhani S J, Kumar A S, Tu Q and Wang H 2019 *Int. J. Mech. Sci.* **159** 459-66